Available online at www.sciencedirect.com
SCIENCE DIRECT®
Journal of Organometallic Chemistry 691 (2006) 898–906
Journal of Organometallic Chemistry
www.elsevier.com/locate/jorganchem

Mixed μ-phosphido or μ-thiolato μ-halo-dimolybdenum(III) compounds $[Mo_2Cp_2(\mu\text{-}SMe)_2(\mu\text{-}X)(\mu\text{-}Y)]$ ($X = PPh_2$, $Y = Cl$; $X = SCH_3$, $Y = Br$, I): Electrochemical and structural comparisons – The X-ray structure of $[\{Mo_2Cp_2Br(\mu\text{-}O)(\mu\text{-}SMe)_2\}_2(\mu\text{-}MoO_4)]$

Christine Le Roy [a], François Y. Pétillon [a], Kenneth W. Muir [b], Philippe Schollhammer [a,*], Jean Talarmin [a]

[a] UMR CNRS 6521, Chimie, Electrochimie Moléculaires et Chimie Analytique, UFR Sciences et Techniques, Université de Bretagne Occidentale, CS 93837, 29238 Brest-cedex 3, France
[b] Chemistry Department, University of Glasgow, Glasgow G12 8QQ, UK

Received 6 September 2005; received in revised form 7 October 2005; accepted 21 October 2005
Available online 1 December 2005

Abstract

Mixed μ-phosphido or μ-thiolato μ-halo-dimolybdenum(III) compounds $[Mo_2Cp_2(\mu\text{-}SMe)_2(\mu\text{-}X)(\mu\text{-}Y)]$ ($X = PPh_2$, $Y = Cl$ (**1**); $X = SCH_3$, $Y = Br$ (**3**), I(**4**)) have been studied. Syntheses and X-ray structures of the new bromo and iodo analogues of $[Mo_2Cp_2(\mu\text{-}SMe)_3(\mu\text{-}Cl)]$ (**2**) are reported. While preparing **3** a side-product **5** was obtained and structurally characterised as the Mo_5 system $[\{Mo_2Cp_2Br(\mu\text{-}O)(\mu\text{-}SMe)_2\}_2(\mu\text{-}MoO_4)]$, containing a $\{Mo^{IV}\text{–}Mo^{IV}\text{–}O\text{–}(Mo^{VI}O_2)\text{–}O\text{–}Mo^{IV}\text{–}Mo^{IV}\}$ unit. The influence of the bridging groups on the structures and electrochemical behaviour of the complexes $[Mo_2Cp_2(\mu\text{-}SMe)_2(\mu\text{-}X)(\mu\text{-}Y)]$ **1**–**4** has been investigated. In MeCN–$[NBu_4][PF_6]$ the first oxidation of $[Mo_2Cp_2(\mu\text{-}SMe)_2(\mu\text{-}PPh_2)(\mu\text{-}Cl)]$ (**1**) is quasi-reversible, contrasting with the essentially irreversible first oxidation of the thiolate analogue $[Mo_2Cp_2(\mu\text{-}SMe)_3(\mu\text{-}Cl)]$ (**2**) under similar conditions. The effects of lowering the temperature or increasing the scan rate on the oxidation of **1** were examined: the initial quasi-reversible oxidation at first became irreversible but at still higher scan rates or lower temperatures the oxidation was again quasi-reversible. This suggests that the oxidation of **1** in MeCN is followed by reversible coordination of acetonitrile to afford the species $[Mo_2Cp_2(\mu\text{-}SMe)_2(\mu\text{-}PPh_2)(Cl)(MeCN)]^+$ ($\mathbf{7}^+$). Cyclic voltammetry of $[Mo_2Cp_2(\mu\text{-}SMe)_3(\mu\text{-}Y)]$($Y = Br$ (**3**) or I (**4**)) showed two quasi-reversible diffusion-controlled oxidation steps in CH_2Cl_2–$[NBu_4][PF_6]$ or thf–$[NBu_4][PF_6]$. In acetonitrile, the fast loss of the halide ligands results in the formation of $[Mo_2Cp_2(\mu\text{-}SMe)_3\text{-}(MeCN)_2]^+$ species.

Keywords: Molybdenum; Dinuclear complexes; Bromo and iodo bridges; Cyclopentadienyl; Oxo ligand; Thiolate; Crystal structure; Electrochemical behaviour

1. Introduction

If the potential of dinuclear organometallic systems as catalysts for molecular activation is ever to be fully developed, it is essential to understand and predict how different ligands control the activity of these systems [1]. For example, choosing a ligand with different electronic or steric properties may induce discrimination between substrates and alter the activity and selectivity of substrate-binding sites. Finding the parameters which favour coordination and activation of a given substrate is a difficult task because reactions often depend on a delicate balance between the electronic and steric properties of the metallic

* Corresponding author.
E-mail addresses: françois.petillon@univ-brest.fr (F.Y. Pétillon), ken@chem.gla.ac.uk (K.W. Muir), schollha@univ-brest.fr (P. Schollhammer), jean.talarmin@univ-brest.fr (J. Talarmin).

0022-328X/$ - see front matter © 2005 Elsevier B.V. All rights reserved.
doi:10.1016/j.jorganchem.2005.10.033

framework and the substrate. These considerations led us previously to study (a) the influence of C_5R_5 rings (R = H, Me) on the electrochemistry and reactivity of $\{Mo_2(C_5R_5)_2(\mu\text{-}SR)_2\}$ systems [2] and (b) the effect of terminal L ligands (RNC, CO, RCN) on nucleophilic and electrophilic additions to complex cations of general type $[Mo_2Cp_2(\mu\text{-}SMe)_3L_2]^+$ [3]. Subsequently, the formation of the μ-phosphido compound $[Mo_2Cp_2(\mu\text{-}SMe)_2(\mu\text{-}PPh_2)(\mu\text{-}Cl)]$ (**1**) when $[Mo_2Cp_2(\mu\text{-}SMe)_3(\mu\text{-}Cl)]$ (**2**) is treated with $HPPh_2$ [4] allowed us to investigate the effect of varying a single μ-X bridging group in bis-cyclopentadienyl derivatives $[Mo_2Cp_2(\mu\text{-}SMe)_2(\mu\text{-}X)(\mu\text{-}Cl)]$ (X = PPh_2, SCH_3). We concluded that the activity of these complexes depends essentially on the lability of the μ-chloro group [5]. In this context we have shown by single-crystal X-ray analysis of **1** that the PPh_2 group is *trans* to chloride; this implies that the conversion of **2** to **1** exclusively involves replacement of the thiolate bridge *trans* to μ-Cl [6]. In addition, investigation of the reactions of **1** and **2** with borohydride revealed that the different activity of the two compounds could be rationalised in term of the differing *trans*-effect of μ-PPh_2 and μ-SMe groups (Scheme 1) [6].

We now attempt to confirm these conclusions by showing from the electrochemical behaviour of $[Mo_2Cp_2(\mu\text{-}SMe)_2(\mu\text{-}PPh_2)(\mu\text{-}Cl)]$ (**1**) that the lability of the μ-chloro bridge depends on the nature of the *trans* bridging group. To extend the scope of this work we have synthesised $[Mo_2Cp_2(\mu\text{-}SMe)_3(\mu\text{-}X)]$ (X = Br (**3**), I (**4**)), the bromo and iodo analogues of **2**, in order to compare their electrochemical behaviour and structural characteristics with those of **1** and **2**. The X-ray structure of a novel Mo_5 system $[\{Mo_2Cp_2Br(\mu\text{-}O)(\mu\text{-}SMe)_2\}_2(\mu\text{-}MoO_4)]$ (**5**), formed as a by-product in the synthesis of **3**, is also reported.

2. Results and discussion

2.1. Syntheses of $[Mo_2Cp_2(\mu\text{-}SMe)_3(\mu\text{-}Y)]$ (Y = Br (3), I (4))

Red solutions of $[Mo_2Cp_2(\mu\text{-}SMe)_3(MeCN)_2]BF_4$ (**6**) [5] in dichloromethane were treated with 1.2 equivalents of $[Bu_4N]Br$ or $[Bu_4N]I$ at room temperature in the presence of zinc dust to give green solutions of complexes **3** or **4** (Scheme 2). ^1H NMR spectra in $CDCl_3$ showed that **3** and **4** were each formed as a mixture of two isomers (**3a**/**3b** ratio: 70/30; **4a**/**4b** ratio: 85/15) which displayed the sets of resonances typical of a symmetrical $\{Mo_2Cp_2(\mu\text{-}SMe)_3\}$ core. The observed isomerism, which is common in tris(thiolato)-bridged complexes [1], probably arises from different orientations (*syn*/*anti*) of the *S*-methyl groups. Addition of 1 equivalent of HBF_4–Et_2O to solutions of **3** or **4** in CH_2Cl_2 resulted in one-electron oxidation of these complexes. The purple, paramagnetic derivatives $[Mo_2Cp_2(\mu\text{-}SMe)_3(\mu\text{-}Y)]BF_4$ (Y = Br ($\mathbf{3}^+$), I ($\mathbf{4}^+$)) were isolated by precipitation with diethylether and characterised by elemental analysis.

2.2. The crystal structures of $[Mo_2Cp_2(\mu\text{-}SMe)_3(\mu\text{-}Y)]$ (Y = Br (3), I (4))

Single crystals of **3** and **4** were obtained from Et_2O solution. The resulting molecular structures are compared with those of **1** and **2** [6] in Table 1. In the asymmetric unit of **3** there are three independent but structurally equivalent molecules (A, B and C). Since the bridging groups of B and C are disordered our discussion will focus on the ordered molecule A which is shown in Fig. 1. The structure of **4** involves two independent, structurally equivalent molecules, A and B, both of which are disordered. The major sites of each (occupancies 80% and 94%) display essentially identical bond lengths and angles (Table 1). Molecule A is shown in Fig. 2.

The molecules **1**–**4** belong to a well-established group in which the Mo–Mo bond of a linear Cp–Mo^{III}–Mo^{III}–Cp moiety is supported by four bridging ligands. As is usual in this group of compounds, the bridges in **1**–**4** are all nearly symmetrical. In **3** (and also in **1** and **2** [6]) the SMe groups *cis* to the μ-Y bridge are *syn*, with the methyl groups adjacent to Y; in **4** the alternative *anti* arrangement of these methyl groups is found. The Mo–Mo bond lengths in Table 1 are nearly constant and evidently are insensitive to the nature of the bridging groups. Mo–Br

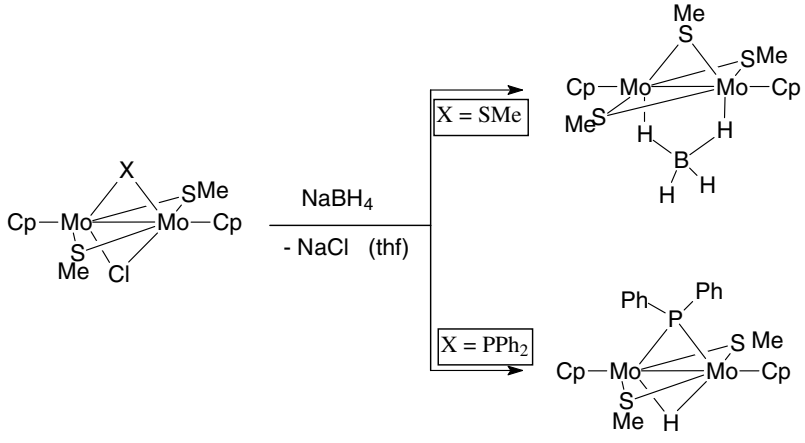

Scheme 1.

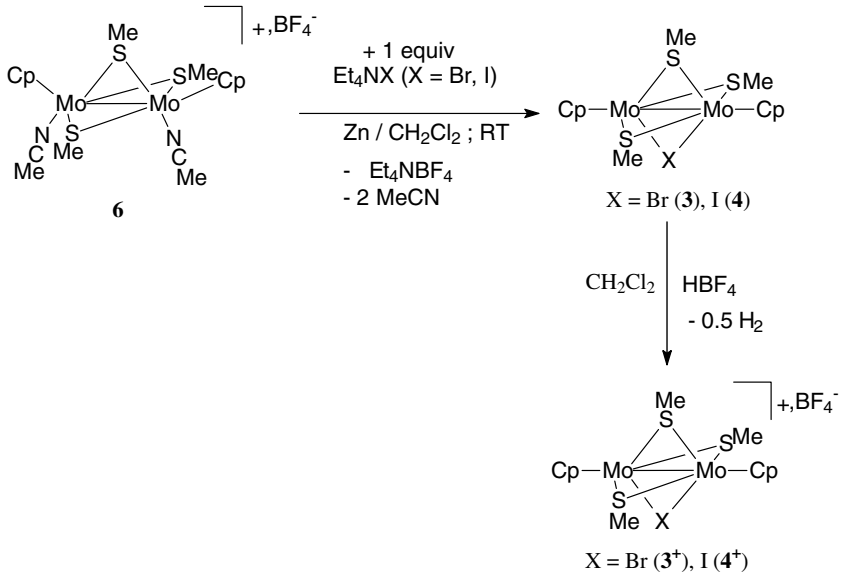

Scheme 2.

Table 1
Selected bond lengths (Å) and angles (°) for the $[Mo_2Cp_2(\mu\text{-SMe})_2(\mu\text{-X})(\mu\text{-Y})]$ complexes **1** (X = PPh_2) [6], **2** (X = SMe) [6], **3** (X= SMe) and **4** (X = SMe)[a]

	1 (Y = Cl; E = P)	**2** (Y = Cl; E = S3)	**3** (Y = Br; E = S3)[b]	**4** (Y = I; E = S3)[c]	
				A	B
Mo1–Mo2	2.627(1)	2.601(1)	2.609(1)	2.629(1)	2.629(1)
Mo1–Y1	2.548(3)	2.481(3)	2.644(1)	2.829(1)	2.829(1)
Mo2–Y1	2.524(3)	2.486(3)	2.632(1)	2.827(1)	2.831(1)
Mo1–S_α	2.454(3)	2.452(3)	2.504(2)	2.437(2)	2.465(2)
Mo2–S_α	2.475(3)	2.458(3)	2.487(2)	2.450(2)	2.461(2)
Mo1–S_β	2.454(3)	2.465(3)	2.444(2)	2.476(2)	2.464(2)
Mo2–S_β	2.471(3)	2.476(3)	2.448(2)	2.506(2)	2.476(2)
Mo1–E	2.398(3)	2.449(3)	2.447(3)	2.442(2)	2.429(2)
Mo2–E	2.394(3)	2.455(3)	2.446(2)	2.433(2)	2.441(2)
Mo1–Y1–Mo2	62.4(1)	63.2(1)	59.3(1)	55.4(1)	55.4(1)
Mo1–S_α–Mo2	64.4(1)	64.0(1)	63.0(1)	65.1(1)	64.5(1)
Mo1–S_β–Mo2	64.5(1)	63.5(1)	64.5(1)	63.7(1)	64.3(1)
Mo1–E–Mo2	66.5(1)	64.1(1)	64.5(1)	65.3(1)	65.4(1)

[a] Relative to Mo1 or Mo2 S_α and S_β are mutually *trans* as are Y and E.
[b] Values are exclusively for the ordered molecule A.
[c] Sites A and B have respective occupancies of 0.799(1) and 0.944(1).

and Mo–I lengths in **3** and **4** compare well with those found in other dimolybdenum(III) compounds [7a,7b,7c,7d]. The mean Mo–Y distances in **2**–**4** of 2.48, 2.64 and 2.83 Å for Y = Cl, Br and I follow nearly exactly the trend of the respective Pauling covalent radii – 0.99, 1.14 and 1.33 Å [7e]. In **2**–**4** there is no evidence that changing Y influences the *trans* Mo–S bond length; however, the mean Mo–S (*trans* to Y) distance of 2.443(3) Å is marginally less than the mean Mo–S (*trans* to S) distance of 2.467(5) but this conclusion must be regarded as tentative in view of the variability of Mo–S distances in these systems. In contrast, the *trans* lengthening effect of PPh_2 compared with SMe on Mo–Cl bonds is clearly evident when the mean Mo–Cl distance in **1** (2.53 Å) is compared with that in **2** (2.48 Å).

*2.3. X-ray structure of [{$Mo_2Cp_2Br(\mu\text{-}O)(\mu\text{-}SMe)_2$}$_2$($\mu$-$MoO_4$)] (**5**)*

During attempts to get single crystals of **3** CH_2Cl_2–Et_2O solutions afforded, after about one month, two types of crystal which had the same colour but different habits. Needle-shaped crystals were found to consist of the μ-bromo compound (**3**). X-ray analysis of a plate-shaped crystal revealed the unexpected structure of a mixed-valence Mo(IV)–Mo(VI) species **5** (Fig. 3). The molecular structure of **5** has exact C_2 symmetry and consists of two identical $\{Mo_2Cp_2Br(\mu\text{-SMe})_2(\mu\text{-O})\}$ units linked by a $\{MoO_4^{2-}\}$ group (Chart 1).

The close analogy between the structural characteristics of the triply-bridged $\{Mo_2Cp_2Br(\mu\text{-SMe})_2(\mu\text{-O})\}$ core

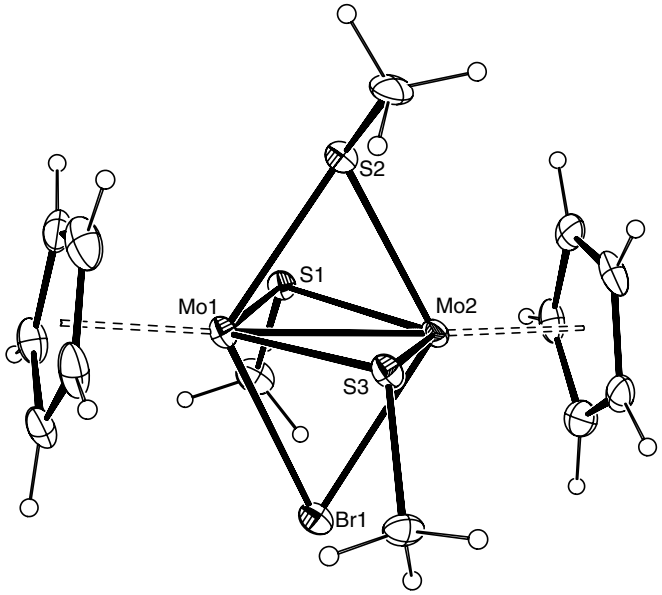

Fig. 1. A drawing of ordered molecule A in crystals of **3**. 20% Thermal ellipsoids are shown here in and in Figs. 2 and 3.

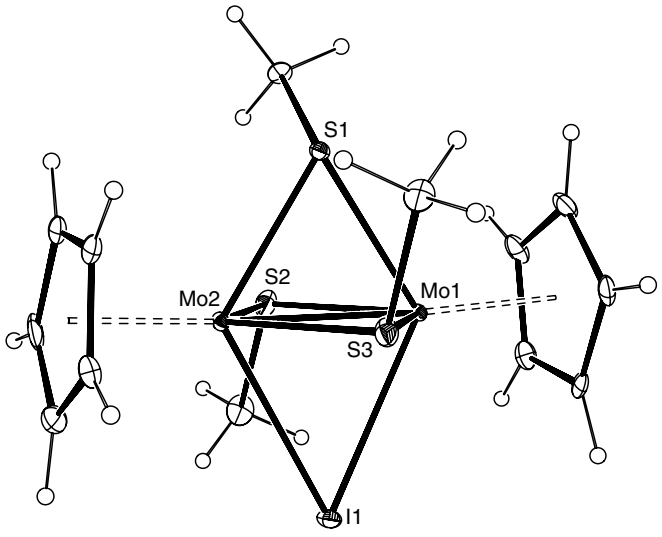

Fig. 2. A view of molecule A in crystals of **4**. Disorder is not shown to aid clarity.

of **5** and that of $[Mo_2Cp^*_2Br_2(\mu\text{-SMe})(\mu\text{-Br})(\mu\text{-O})]$ ($Cp^* = C_5Me_5$) [8] is evident from Table 2. Each metal centre in these complexes attains a four-legged piano stool coordination. A terminal ligand forms one of the legs and the remaining three are supplied by ligands which symmetrically bridge a rather long Mo–Mo bond (cf. 2.728(1) Å in **5** with 2.60–2.63 in **1**–**4**). Though normal electron counting rules require the presence of a Mo–Mo double bond in **5**, it is known [8,9] that a single frontier orbital is mainly responsible for the Mo–Mo bonding in such complexes. Because of this the presence of long Mo–Mo bonds in **5** and $[Mo_2Cp^*_2Br_2$-

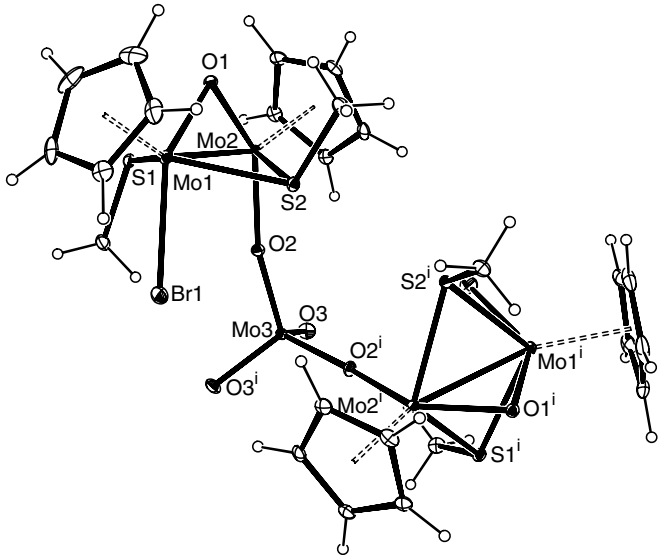

Fig. 3. A view of compound **5**.

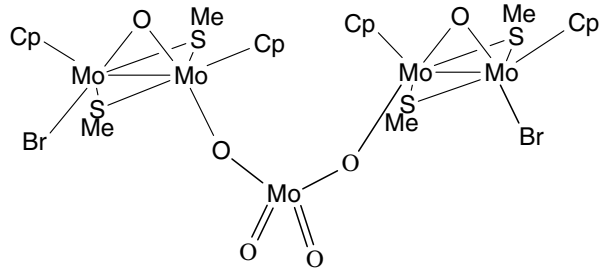

5

Chart 1.

Table 2
Comparison of selected bond lengths (Å) and angles (°) for **5** with those in $[Mo_2Br_2Cp^*_2(\mu\text{-SMe})(\mu\text{-Br})(\mu\text{-O})]$ (A) [8] and in the $\{Mo^{II}\text{–O–}Mo^{VI}O_2\text{–O–}Mo^{II}\}$ containing system (B) $[\{Mo(\eta^3\text{-}C_3H_4Me)(Phen)(CO)_2\}_2(\mu\text{-}MoO_4)]$ [10b]

	5	A	B
Mo1–Mo2	2.728(1)	2.755(1)	
Mo1–Br1	2.574(1)	2.559(2)	
		2.552(2)	
Mo1–S1	2.457(1)	2.457(3)	
Mo1–S2	2.432(1)		
Mo2–S1	2.479(1)	2.474(3)	
Mo2–S2	2.443(1)		
Mo1–O1	1.944(2)	1.914(7)	
Mo2–O1	1.927(2)	1.907(6)	
Mo3–O3	1.723(2)		1.731(3), 1.739(3)
Mo3–O2	1.810(2)		1.795(3), 1.797(3)
Mo2–O2	1.994(2)		2.107(3), 2.070(4)
Mo1–O1–Mo2	89.6(1)	92.3(3)	
Mo1–S1–Mo2	67.1(1)	68.0(1)	
Mo1–S2–Mo2	68.1(1)		
Mo3–O2–Mo2	166.1(1)		156.8(2), 156.8 (2)
Br1–Mo1–Mo2	96.3(1)	100.7(1)	
		99.8 (1)	

(μ-SMe)(μ-Br)(μ-O)] is not surprising – see [8,9] for further discussion of this point. Metal–ligand distances in **5** are unexceptional.

The distinctive structural feature of the molecule is the $\{Mo^{IV}–O–Mo^{VI}O_2–O–Mo^{IV}\}$ unit. There are relatively few reports of complexes in which an MoO_4^{2-} unit is the *only* bridge between two molybdenum fragments [10]. The bridging MoO_4^{2-} group in **5** has regular tetrahedral coordination at Mo3, with O–Mo3–O angles of 107.9(2)–111.9(1)°. The Mo3–O bonds to bridging O are longer than the terminal Mo–O bonds (cf. 1.810(2) and 1.723(2) Å). As can be seen from Table 2 these results agree with those for [{Mo(η³-C_3H_4Me)(Phen)(CO)$_2$}$_2$(μ-MoO_4)] [10b]. Similar distances are found in related compounds [10] but the Mo3–O2–Mo2 angle of 166.1(1)° in **5** seems unusually large (see Table 2).

Yields of **5** cannot be determined, its formation from **3** is surprising since it requires the cleavage of several metal–ligand bonds (Mo–Cp, Mo–SMe, Mo–Br) in the presence of water or dioxygen and recombination of the resulting bimetallic and monometallic fragments. The mechanism of the reaction is not known and it has not yet been possible to specify the experimental conditions required for the reproducible conversion of **3** into **5**. For this reason further analytical and spectroscopic data for **5** are not available. A recent discussion of the factors which favour formation of oxo-stabilised complexes of molybdenum in high oxidation states [11] has emphasised the wide variety of polynuclear cyclopentadienyl oxo-molybdenum species which may exist. The similarities we have noted between **5** and [$Mo_2Cp^*_2Br_2$(μ-SMe)-(μ-Br)(μ-O)] ($Cp^* = C_5Me_5$) [8] suggest that reaction of the latter with MoO_4^{2-} might lead to species analogous to **5**. This and similar reactions appear worth further investigation.

2.4. Electrochemical studies

2.4.1. Electrochemical behaviour of [Mo_2Cp_2(μ-SMe)$_2$-(μ-PPh_2)(μ-Cl)] (**1**)

The cyclic voltammetry (CV) of [Mo_2Cp_2(μ-SMe)$_2$(μ-PPh_2)(μ-Cl)] (**1**) in CH_2Cl_2–[NBu_4][PF_6] showed that the complex underwent two oxidation processes. From the usual diagnostic criteria ($i_p/v^{1/2} = f(v)$, i_p^c/i_p^a close to 1 for $0.02\ V\ s^{-1} \leqslant v \leqslant 1\ V\ s^{-1}$) [12,13] both oxidations are assigned as quasi-reversible ($\Delta E_p > 60$ mV), diffusion-controlled one-electron steps with $E_{1/2}^{ox1} = -0.29$ V and $E_{1/2}^{ox2} = 0.47$ V (Table 3). **1** also underwent two oxidation steps (as well as an irreversible reduction) in thf–[NBu_4][PF_6], but only the first one is reversible with $E_{1/2}^{ox1} = -0.29$ V. Controlled-potential electrolysis of **1** at 0 V (Pt anode, CH_2Cl_2–[NBu_4][PF_6] and thf–[NBu_4][PF_6]) produced $\mathbf{1}^+$ quantitatively [14] after the transfer of ca $0.9\ F\ mol^{-1}$ **1**.

In MeCN–[NBu_4][PF_6], the first oxidation of **1** appeared as a quasi-reversible system with $E_{1/2}^{ox} = -0.34$ V (Table 3, Fig. 4(a)), which contrasts with the essentially irreversible first oxidation of **2** under similar conditions ($v \leqslant 0.4\ V\ s^{-1}$, [5]; see Fig. 6(a) in supplementary material). However, a small irreversible reduction peak was also observed around −0.6 V for **1**. In addition, it should be noted that another species was detected by its reversible oxidation at $E_{1/2}^{ox} = -0.11$ V and that it has been formulated as [Mo_2Cp_2(μ-SMe)$_2$(μ-PPh_2)(MeCN)$_2$]$^+$ (**6′**). Its formation may arise from a slow chloride loss from [Mo_2Cp_2(μ-SMe)$_2$-(μ-PPh_2)(μ-Cl)] (**1**), like the similar loss shown by the tris(μ-thiolato) series [5]. This product could not be isolated because of the lability of the MeCN ligands but its formulation is supported by the observation that its reversible oxidation replaced the redox processes of **1** when K[PF_6] or HBF_4 was added to the solution.

Table 3
Redox potentials of the complexes measured by cyclic voltammetry (vitreous carbon electrode, $v = 0.2\ V\ s^{-1}$)[a]

Complex	Solvent	E_p^{red}	$E_{1/2}^{ox1}$	$E_{1/2}^{ox2}$
[Mo_2Cp_2(μ-SMe)$_2$(μ-PPh_2)(μ-Cl)] (**1**)	thf		−0.29	0.46 (irr)
	CH_2Cl_2		−0.29	0.47
	MeCN (RT)		−0.34[b]	
	MeCN (−45 °C)		−0.30	
[Mo_2Cp_2(μ-SMe)$_2$(μ-PPh_2)(MeCN)$_2$]$^+$ (**6′**)	MeCN		−0.11	
[Mo_2Cp_2(μ-SMe)$_2$(μ-PPh_2)(Cl)(MeCN)]$^+$ (**7**$^+$)	MeCN	−0.6		
[Mo_2Cp_2(μ-SMe)$_3$(μ-Cl)] (**2**)	MeCN (−45 °C)		−0.44	0.32
[Mo_2Cp_2(μ-SMe)$_3$(μ-Br)] (**3**)	thf		−0.38	0.31
	CH_2Cl_2		−0.42	0.42
	MeCN (0 °C)		−0.42	0.33
[Mo_2Cp_2(μ-SMe)$_3$(μ-I)] (**4**)	thf		−0.45	0.26
	CH_2Cl_2		−0.44	0.42
	MeCN (0 °C)		−0.40	0.32

[a] Potentials are in volts relative to the Fc^+/Fc couple; irr: irreversible.
[b] CE process.

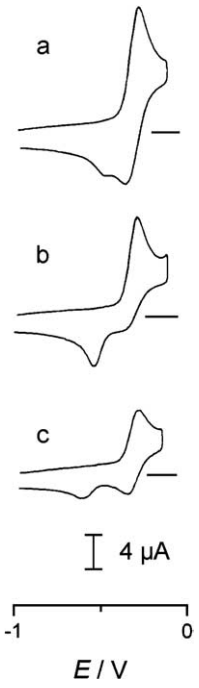

Fig. 4. Cyclic voltammetry of $[Mo_2Cp_2(\mu\text{-}SMe)_2(\mu\text{-}PPh_2)(\mu\text{-}Cl)]$ (**1**) (ca. 1 mM) at (a) 15 °C, (b) −11 °C, and (c) −45 °C (MeCN–$[NBu_4][PF_6]$, vitreous carbon electrode, scan rate $v = 0.2$ V s^{-1}).

The CV of **1** was examined at different scan rates and different temperatures in MeCN in order to determine the reason for the differing behaviour of **1** and **2**. Whereas the oxidation of **1** was quasi-reversible for $0.02 \text{ V s}^{-1} \leqslant v \leqslant 0.2 \text{ V s}^{-1}$ (room temperature), it became markedly irreversible for scan rates in the range 3–5 V s^{-1}. Under these conditions the major product detected on the return scan was characterised by an irreversible reduction around −0.6 V. Increasing the scan rate up to 20–30 V s^{-1} led to further modifications of the CV: the oxidation became quasi-reversible again ($E^{ox1}_{1/2} = -0.29$ V, Table 3). The large peak-to-peak separation measured under these conditions ($\Delta E_p = 151$ mV for $v = 30$ V s^{-1} while $\Delta E_p = 70$ mV for $v = 0.02$ V s^{-1}) can be assigned, at least partly, to uncompensated solution resistance.

Similar effects on the reversibility of the oxidation of **1** were obtained by lowering the temperature. For a common scan rate of 0.2 V s^{-1}, the oxidation which is quasi-reversible at room temperature (Fig. 4(a)) became irreversible around −10 °C (Fig. 4(b)). At still lower temperature (−45 °C), a quasi-reversible couple was again observed (Fig. 4(c)).

Taken together, these observations demonstrate that the electrochemical oxidation of **1** in MeCN is followed by a *reversible* chemical reaction. By analogy with the processes reported for $[Mo_2Cp_2(\mu\text{-}SMe)_3(\mu\text{-}Cl)]$ [5], this was assigned to the coordination of a solvent molecule to $\mathbf{1}^+$ affording $[Mo_2Cp_2(\mu\text{-}SMe)_2(\mu\text{-}PPh_2)(Cl)(MeCN)]^+$ ($\mathbf{7}^+$) (Scheme 3) which is detected by its irreversible reduction around −0.6 V. We suggest that the follow-up chemical step is made irreversible by increasing the scan rate to 3–5 V s^{-1} or decreasing the temperature to ca −10 °C through suppression of the backward reaction (solvent loss, step c in Scheme 3). The forward reaction (solvent binding: step b in Scheme 3) is substantially but not completely suppressed at higher scan rates ($v > 20$ V s^{-1} at room temperature) or lower temperatures ($T = -45$ °C for $v = 0.2$ V s^{-1}) (Fig. 4(c)). Under these conditions the major electrochemical process detected

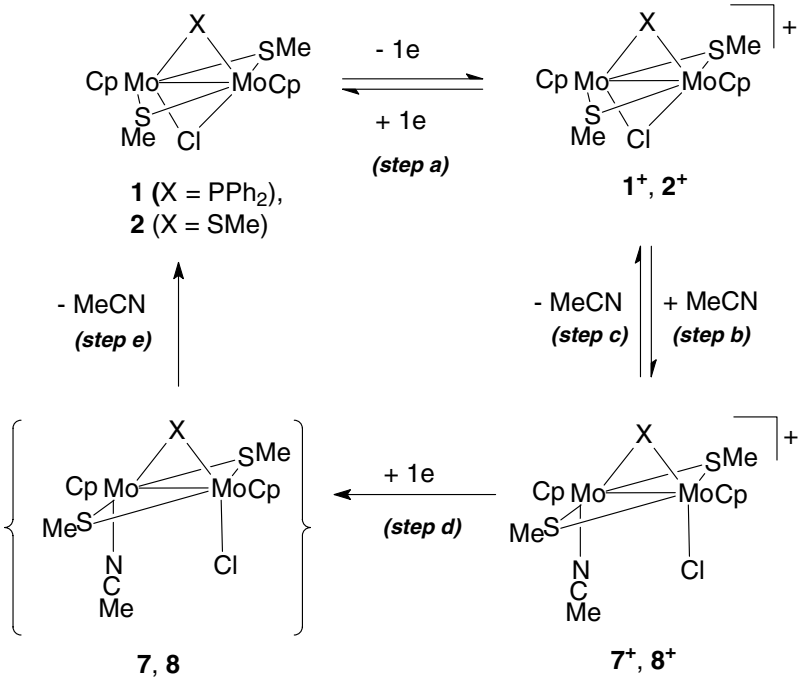

Scheme 3.

by CV corresponds to the reversible one-electron oxidation of **1** (Fig. 4(c); Scheme 3, step a). The reduction of $\mathbf{7}^+$ remains completely irreversible under any conditions of scan rate or temperature used in this study, showing that loss of MeCN (step e) from **7** (undetected) cannot be suppressed.

Controlled-potential oxidation of **1** in MeCN–$[NBu_4][PF_6]$ at room temperature ($E = -0.2$ V, Pt anode) was complete after the transfer of 0.9 F mol^{-1} **1**. The temperature-dependence of the CV of the oxidised solution is shown in Fig. 5(a)–(c). The quasi-reversible system with $E^{red}_{1/2} = -0.34$ V (Fig. 5(a), 13 °C) arises from a CE mechanism [12,13]; loss of MeCN from $\mathbf{7}^+$ produced $\mathbf{1}^+$ (Scheme 3, step c) which reduced at a potential less negative than $\mathbf{7}^+$. CVs in Fig. 5(b) and (c) demonstrate that the major product in the solution at lower temperatures is $\mathbf{7}^+$, as is shown by the presence of the irreversible reduction around −0.6 V, which regenerates the starting material (Scheme 3, steps d and e).

The CVs of **1** at ca −10 and − 45 °C ($v = 0.2$ V s^{-1}) are thus *qualitatively* similar to those of **2** at room temperature (compare Figs. 4(b) and 6(a) in supplementary material), and −10 °C (Figs. 4(c) and 6(b) in supplementary material) respectively, suggesting that the difference in the electrochemistry of **1** and **2** arises principally from the magnitude of the rate constants of the chemical steps b and c (Scheme 3). It should be noted that solvent binding to $\mathbf{2}^+$ can be completely suppressed (at −45 °C, Fig. 6(c)), whereas the formation of some acetonitrile-chloro complex $[Mo_2Cp_2(\mu\text{-}SMe)_2(\mu\text{-}PPh_2)(Cl)(MeCN)]^+$ ($\mathbf{7}^+$) was still observed at the same temperature (Fig. 4(c)). This indicates that the rate constant for step b (Scheme 3) is larger for $\mathbf{1}^+$ than for $\mathbf{2}^+$. It is worth noting that the reduction of $[Mo_2Cp_2(\mu\text{-}SMe)_3(Cl)(MeCN)]^+$ ($\mathbf{8}^+$) which occurs around −0.75 V according to an EC mechanism at room temperature [4] (Fig. 7(a) in supplementary material; steps d and e, Scheme 3,), is turned to a CE process upon warming the solution to ca 50 °C, due to an increase in the rate constant of the forward reaction (step c, Scheme 3), which shifts the equilibrium towards $\mathbf{2}^+$.

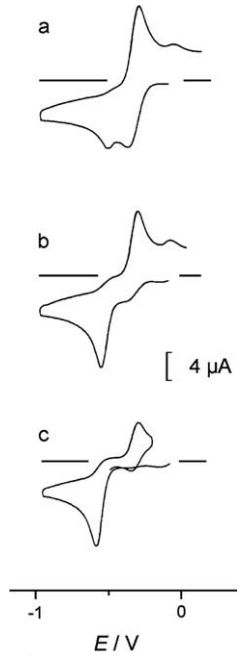

Fig. 5. Cyclic voltammetry of $[Mo_2Cp_2(\mu\text{-}SMe)_2(\mu\text{-}PPh_2)(\mu\text{-}Cl)]$ (**1**) (0.7 mM) after controlled-potential oxidation at −0.2 V, at (a) 13 °C, (b) −14 °C, and (c) −45 °C (MeCN–$[NBu_4][PF_6]$, vitreous carbon electrode, scan rate $v = 0.2$ V s^{-1}).

2.4.2. Electrochemical behaviour of $[Mo_2Cp_2(\mu\text{-}SMe)_3(\mu\text{-}Y)]$ (Y = Br (3) or I (4))

Cyclic voltammetry of $[Mo_2Cp_2(\mu\text{-}SMe)_3(\mu\text{-}Y)]$ (Y = Br (**3**) or I (**4**)) has also been investigated in order to check the influence of the halide ligand on the processes previously reported [5]. Like **1** and **2**, complexes **3** and **4** showed two quasi-reversible ($\Delta E_p > 60$ mV), diffusion-controlled oxidation steps in CH_2Cl_2–$[NBu_4][PF_6]$ or thf–$[NBu_4][PF_6]$ (Table 3). In acetonitrile, loss of the halide ligand is faster when Y = Br and I than when Y = Cl. Indeed, the first oxidation of the starting material ($E^{ox1}_{1/2} = -0.42$ V, Y = Br; $E^{ox1}_{1/2} = -0.40$ V, X = I) was rapidly replaced by that of **6**. Loss of the Y ligand, although it is slowed down at 0 °C, impedes any study of the effect of the halide bridge on the processes described in Scheme 3 for Y = Br and I.

3. Conclusions

The synthesis and characterisation of the derivatives $[Mo_2Cp_2(\mu\text{-}SMe)_3(\mu\text{-}Y)]$ (Y = Br (**3**) or I (**4**)) has allowed us to compare the structures and reactivities of the complexes **1**–**4**. Crystals of the new compound **5** were obtained when recrystallising **3**. Their X-ray analysis revealed an unexpected mixed-valence Mo(IV)–Mo(VI) structure based on two identical $\{Mo_2Cp_2Br(\mu\text{-}SMe)_2(\mu\text{-}O)\}$ units linked by a $\{MoO_4^{2-}\}$ group.

The electrochemical studies of the compounds $[Mo_2Cp_2(\mu\text{-}SMe)_2(\mu\text{-}PPh_2)(\mu\text{-}Cl)]$ (**1**) and $[Mo_2Cp_2(\mu\text{-}SMe)_3(\mu\text{-}Y)]$ (Y = Br (**3**) or I (**4**)) complement our earlier work on deprotection of a coordination site in the chloro-bridged bimetallic system $[Mo_2Cp_2(\mu\text{-}SMe)_3(\mu\text{-}Cl)]$ (**2**) [5]. The present work shows that in acetonitrile the complexes **3** (Y = Br) and **4** (Y = I) lose readily the halide ligand, giving the bis-nitrile ionic species $[Mo_2Cp_2(\mu\text{-}SMe)_3(MeCN)_2]^+$. The new results in part relate to processes in which ligands are gained or lost as the chloride bridge in $[Mo_2Cp_2(\mu\text{-}SMe)_2(\mu\text{-}X)(\mu\text{-}Cl)]$ (X = SMe, PPh_2) complexes opens or closes; they establish that the kinetics of such reactions depend on the nature of the bridging ligand (SMe or PPh_2) *trans* to the μ-Cl group. Apart from their effect on the ability of the complex to donate electrons, the substitution of PPh_2 for SMe at the apical bridging position changes the magnitude of the rate constants for binding or loss of the acetonitrile substrate (with concomitant switch between bridging and terminal roles for the the chloride ligand). Our results suggest that

these rates constants are larger for the phosphido compounds than for their thiolato analogues. The phosphido complexes thus appear "hotter" than their tris(thiolato)-bridged analogues and able to react under milder conditions. This is consistent with other results we recently reported [6].

4. Experimental

4.1. General

All reactions were performed under an atmosphere of argon or dinitrogen using conventional Schlenk techniques. Solvents were deoxygenated and dried by standard methods. Literature methods were used for the preparation of $[Mo_2Cp_2(\mu\text{-}SMe)_2(\mu\text{-}PPh_2)(\mu\text{-}Cl)]$ (**1**) [4] and $[Mo_2Cp_2(\mu\text{-}SMe)_3(MeCN)_2]BF_4$ (**6**) [6]. All other reagents were purchased commercially. Chemical analyses were performed by the Centre de Microanalyses du CNRS, Vernaison (France). The NMR spectra (^1H), in $CDCl_3$ solutions, were recorded at room temperature with a Bruker AC 300 or AMX 400 spectrometers and were referenced to $SiMe_4$. The preparation and the purification of the supporting electrolyte $[NBu_4][PF_6]$, the electrochemical equipment were as described previously [15]. All the potentials (text, tables, figures) are quoted against the ferrocene–ferrocenium couple; ferrocene was added as an internal standard at the end of the experiments. The mass spectra were measured with a LC–MS ThermoFinnigan spectrometer at the "Laboratoire de Biochimie", Faculté de Médecine (Brest, France).

4.2. Synthesis of complexes $[Mo_2Cp_2(\mu\text{-}SMe)_3(\mu\text{-}Y)]$ (Y = Br (**3**), I (**4**))

A solution of **6** (0.2 g, 0.32 mmol) in CH_2Cl_2 (10 mL) was stirred for 20 min in the presence of a slight excess of $[Bu_4N]Y$ (Y = Br (0.13 g, 0.38 mmol), I (0.14 g, 0.40 mmol)) and of an excess of zinc dust (0.21 g, 0.31 mmol). The solution was then filtered and the solvent evaporated. Compounds $[Mo_2Cp_2(\mu\text{-}SMe)_3(\mu\text{-}Y)]$ were extracted with diethylether (3 × 10 mL) and obtained, after the diethylether was removed in vacuo from the pooled extracts, as green powders (**3**: 0.129 g, 74% yield; **4**: 0.083 g, 44%, yield). In spite of several attempts, no reliable analyses are available for **3** and **4**, however both complexes have been characterised by X-ray analysis of their crystals. Electrospray mass spectroscopy confirmed the structures of **3** and **4**. The observed isotope patterns of the molecular ion peaks at *m/z* 543 and 590 are in good agreement with calculated isotope distribution for **3** and **4**, respectively. Moreover, good analytical data were obtained for their cationic forms $\mathbf{3}^+$ and $\mathbf{4}^+$ (see next section).

^1H NMR ($CDCl_3$, RT, δ): **3a** (70%): 5.42 (s, 10H, C_5H_5), 1.63 (s, 3H, SCH_3), 1.59 (s, 3H, SCH_3), 1.52 (s, 3H, SCH_3); **3b** (30%): 5.41 (s, 10H, C_5H_5), 1.75 (s, 3H, SCH_3), 1.70 (s, 3H, SCH_3), 1.67 (s, 3H, SCH_3); **4a** (85%): 5.37 (s, 10H, C_5H_5), 1.94 (s, 3H, S CH_3), 1.57 (s, 3H, SCH_3), 1.53 (s, 3H, SCH_3); **4b** (15%): 5.36 (s, 10H, C_5H_5), 2.07 (s, 3H, SCH_3), 2.01 (s, 3H, SCH_3), 1.61 (s, 3H, SCH_3).

ESI-MS (*m/z*): **3**: 543 $[M]^+$, 496 $[M - (SCH_3)]^+$, 463 $[M - Br]^+$. **4**: 590 $[M]^+$, 496 $[M - 2(SCH_3)]^+$, 463 $[M - I]^+$.

4.3. Synthesis of complexes $[Mo_2Cp_2(\mu\text{-}SMe)_3(\mu\text{-}Y)]BF_4$ (Y = Br ($\mathbf{3}^+$), I ($\mathbf{4}^+$))

In a typical procedure, 1 equivalent of HBF_4–Et_2O was added to a green solution of $[Mo_2Cp_2(\mu\text{-}SMe)_3(\mu\text{-}Y)]$ (**3**: 0.1 g, 0.18 mmol; **4**: 0.1 g, 0.17 mmol) in CH_2Cl_2 (10 mL) The solution instantly turned purple. It was stirred for 10 m and the volume of the solvent was then reduced under vacuum. Addition of diethyl ether (20 mL) precipitated $[Mo_2Cp_2(\mu\text{-}SMe)_3(\mu\text{-}Y)](BF_4)$ (Y = Br ($\mathbf{3}^+$), I ($\mathbf{4}^+$)) as purple solids ($\mathbf{3}^+$: 0.9 g, 79% yield; $\mathbf{4}^+$: 0.95 g, 82% yield). $\mathbf{3}^+$: Anal Calc. for $C_{13}H_{19}BBrF_4Mo_2S_3$: C, 24.8; H, 3.0; Br, 12.7. Found: C, 24.9; H, 3.1; Br, 12.2%. $\mathbf{4}^+$: Anal Calc. for $C_{13}H_{19}BF_4IMo_2S_3$: C, 23.1; H, 2.8; I, 18.7. Found: C, 22.7; H, 2.9; I, 17.7%.

4.4. Structure analyses of 3–5

All measurements were made at 100 K on a Nonius KappaCCD diffractometer with Mo Kα radiation, $\lambda = 0.71073$ Å. The structures were solved and refined by standard procedures [16]. H atoms were positioned using stereochemical considerations, the orientations of methyl groups being initially obtained from difference maps, and then rode on their parent carbon atoms.

3, $C_{13}H_{19}BrMo_2S_3$, monoclinic, space group $P2_1/c$, $a = 22.2786(3)$ Å, $b = 8.0829(1)$ Å, $c = 28.9381(5)$ Å, $\beta = 104.818(1)°$, $V = 5037.7(1)$ Å^3, $Z = 12$, $T = 100$ K, $R(F) = 0.078$ for 8571 observed reflections, $wR(F^2) = 0.201$ for all 14708 independent reflections with $1.5 < \theta$ (Mo Kα) < 30.1°, $|\Delta\rho| < 3.2$ e$^-$ Å^{-3}. There are three independent molecules, A, B and C, in the asymmetric unit. The SMe and Br bridging groups of molecules B and C are disordered. Disordered H-atoms were not included in the calculations and Cp rings were regular pentagons of side 1.42 Å.

4, $C_{13}H_{19}IMo_2S_3$, triclinic, space group $P\bar{1}$, $a = 9.4246(1)$ Å, $b = 12.7566(2)$ Å, $c = 14.5183(2)$ Å, $\alpha = 92.874(1)$, $\beta = 101.325(1)$, $\gamma = 90.665(1)°$, $V = 1708.93(4)$ Å^3, $Z = 4$, $T = 100$ K, $R(F) = 0.062$ and $wR(F^2) = 0.156$ for all 7698 independent reflections with $2.1 < \theta$(Mo Kα) < 27.6°, $|\Delta\rho| < 3.25$ e$^-$Å^{-3}. The crystals show non-merohedral twinning refined using the HKLF 5 option in SHELXL [16]. The major twin made up 0.740(3) of the specimen. In addition, both independent molecules are disordered, with major site occupancies of 0.799(1) and 0.944(1).

5, $C_{24}H_{32}Br_2Mo_5O_6S_4 \cdot 2CH_2Cl_2$, monoclinic, space group $C2/c$, $a = 20.7726(3)$ Å, $b = 9.1779(1)$ Å, $c = 20.8043(2)$ Å, $\beta = 96.390(1)°$, $V = 3941.67(8)$ Å^3, $Z = 4$, $T = 100$ K, $R(F) = 0.045$ and $wR(F^2) = 0.106$ for all 8661

independent reflections with $2.0 < \theta(\text{Mo K}\alpha) < 35.0°$, $|\Delta\rho| < 3.4$ e Å^{-3}.

Acknowledgements

We thank the CNRS, the EPSRC, Glasgow University and the University of Brest for financial support. We thank Dr. D. Picart for recording ESI-MS.

Appendix A. Supplementary data

Crystallographic information (CIF) files for **3**, **4** and **5** have been deposited with the Cambridge Structural Database. The deposition numbers are CCDC 279843–279845. Supplementary data associated with this article can be found, in the online version, at doi:10.1016/j.jorganchem.2005.10.033.

References

[1] F.Y. Pétillon, P. Schollhammer, J. Talarmin, K.W. Muir, Coord. Chem. Rev. 178–180 (1998) 203, and references therein.
[2] (a) P. Schollhammer, F.Y. Pétillon, R. Pichon, S. Poder-Guillou, J. Talarmin, K.W. Muir, L. Manojlovic-Muir, Organometallics 14 (1995) 2277;
(b) F.Y. Pétillon, S. Poder-Guillou, P. Schollhammer, J. Talarmin, New J. Chem. 21 (1997) 477.
[3] (a) N. Cabon, P.Y. Orain, F.Y. Pétillon, P. Schollhammer, J. Talarmin, K.W. Muir, J. Organomet. Chem. 690 (2005) 4583;
(b) N. Cabon, F.Y. Pétillon, P. Schollhammer, J. Talarmin, K.W. Muir, J. Organomet. Chem. doi:10.1016/j.jorganchem.2005.09.042.
[4] P. Schollhammer, E. Guénin, S. Poder-Guillou, F.Y. Pétillon, J. Talarmin, K.W. Muir, P. Baguley, J. Organomet. Chem. 539 (1997) 193.
[5] F. Barrière, Y. Le Mest, F.Y. Pétillon, S. Poder-Guillou, P. Schollhammer, J. Talarmin, J. Chem. Soc., Dalton Trans. (1996) 3967.
[6] N. Cabon, F.Y. Pétillon, P. Schollhammer, J. Talarmin, K.W. Muir, J. Chem. Soc., Dalton Trans. (2004) 2708.
[7] (a) P.B. Grebenik, M.L.H. Green, A. Izquierdo, V.S.B. Mietwa, K. Prout, J. Chem. Soc., Dalton Trans. (1987) 9;
(b) K. Fromm, E. Hey-Hawkins, Z. Anorg. Allg. Chem. 619 (1993) 261;
(c) J.U. Desai, J.C. Gordon, H.-B. Kraatz, V.T. Lee, B.E. Owens-Waltermire, R. Poli, A.L. Rheingold, C.B. White, Inorg. Chem. 33 (1994) 3752;
(d) J.H. Shin, G. Parkin, Polyhedron 13 (1994) 1489;
(e) L. Pauling, The Nature of the Chemical Bond, Cornell University Press, Ithaca, New York, 1960, p. 224.
[8] S. Poder-Guillou, P. Schollhammer, F.Y. Pétillon, J. Talarmin, K.W. Muir, P. Baguley, Inorg. Chim. Acta 257 (1997) 153, and references therein.
[9] (a) F. Abugideiri, J.C. Fettinger, R. Poli, Inorg. Chim. Acta 229 (1995) 445;
(b) J.C. Green, M.L.H. Green, P. Mountford, M.J. Parkington, J. Chem. Soc., Dalton Trans. (1990) 3407;
(c) D.L. DuBois, W.K. Miller, M. Rakowski DuBois, J. Am. Chem. Soc. 103 (1981) 3429;
(d) W. Tremel, R. Hoffmann, E.D. Jemmis, Inorg. Chem. 28 (1989) 1213.
[10] (a) K. Prout, J.C. Daran, Acta Crystallogr. B 34 (1978) 3586;
(b) C. Borgmann, C. Limberg, L. Zsolnai, Chem. Commun. (1998) 2729;
(c) D. Morales, J. Perez, L. Riera, V. Riera, D. Miguel, M.E.G. Mosquera, S. Garcai-Granda, Chem. Eur. J. 9 (2003) 4132;
(d) L. Contreras, M. Paneque, M. Sellin, E. Carmona, P.J. Pérez, E. Gutiérrez-Puebla, A. Monge, C. Ruiz, New J. Chem. 29 (2005) 109;
(e) G. Schoettel, J. Kress, J. Fischer, J. Osborn, J. Chem. Soc., Chem. Commun. (1988) 914.
[11] R. Poli, Chem. Eur. J. 10 (2004) 332.
[12] (a) A.J. Bard, L.R. Faulkner, in: Electrochemical Methods. Fundamentals and Applications, Wiley, New York, 1980, p. 429 (Chapter 11);
(b) E.R. Brown, R.F. Large, Techniques of Chemistry, in: A. Weissberger (Ed.), Physical Methods of Chemistry, Part IIA, vol. I, Wiley, 1971, p. 423 (Chapter 6).
[13] The parameters i_p and E_p are respectively the peak current and the peak potential of a redox process; $E_{1/2} = (E_p^a + E_p^c)/2$; E_p^a, i_p^a and E_p^c, i_p^c are respectively the potential and the current of the anodic and of the cathodic peak of a reversible process; $\Delta E_p = E_p^a - E_p^c$; an EC process comprises an electron transfer step (E) followed by a chemical reaction (C); in a CE process, the electroactive species are connected by an equilibrium. CV stands for cyclic voltammetry; v (V s^{-1}) is the scan rate in CV experiments.
[14] The yield of the controlled-potential oxidation was calculated by comparing the oxidation peak current of **1** to the reduction peak current of $\mathbf{1}^+$.
[15] J.Y. Cabon, C. Le Roy, K.W. Muir, F.Y. Pétillon, F. Quentel, P. Schollhammer, J. Talarmin, Chem. Eur. J. 6 (2000) 3033.
[16] (a) G.M. Sheldrick, Programs used: SHELX-97, University of Göttingen, Germany, 1998;
(b) WINGX – A windows program for crystal structure analysis L.J. Farrugia, J. Appl. Crystallogr. 32 (1999) 837.